Foam flow investigation in 3D printed porous media: Fingering and gravitational effects

Mohammad Javad Shojaei[1], Kofi Osei-Bonsu[1], Paul Grassia[2], and Nima Shokri*[1]

[1]School of Chemical Engineering and Analytical Science, University of Manchester, Manchester, UK

[2] Department of Chemical and Process Engineering, University of Strathclyde, Glasgow, UK

***Corresponding Author**

Dr. Nima Shokri

School of Chemical Engineering and Analytical Science

Room C26, The Mill

The University of Manchester

Sackville Street, Manchester, M13 9PL, UK

Tel: 0441613063980

Email: nima.shokri@manchester.ac.uk

16Group website: http://personalpages.manchester.ac.uk/staff/nima.shokri/

ABSTRACT

Flow in porous media investigations have shown foam injection have a higher sweep efficiency compare to gas injection. However, fingering of highly mobile gas into the foam bank and separation of fluids (gas and surfactant) resulted by gravity segregation can influence the performance of foam injection project. To the best of our knowledge, this phenomenon has not been investigated experimentally in the literature. In this study, foam injection experiments have been performed in a model oriented in a horizontal and perpendicular orientation with respect to gravity using also different flow rates. High resolution imaging tools were utilized to record displacement process of oil by gas/surfactant/foam. The recorded images enabled us to monitor gas fingering and foam flow dynamics at pore scale. The obtained results highlighted the adverse effect of fingering of highly mobile gas into the foam bank and fluids separation by gravity segregation in the performance of foam project.

KEYWORDS: Foam flow in porous media, Gas Fingering, Gravity segregation, 3D printing technology, Pore-scale visualization

INTRODUCTION

Displacement of fluids with gas and water is a common practice in many industrial applications such as soil remediation, enhanced oil recovery (EOR) and CO2 sequestration. Gravity segregation due to the density difference between displaced and displacing fluids divides the porous medium into three zones I) override zone where only the phase with the lower density exists, II) underride zone where only the phase with the higher density exists and III) the mixed zone where both phases exist simultaneously[1]. This selective movement of fluids inside the porous media causes unstable displacement that influences the reservoir performance[2, 3]. Foam which is a discontinuous gas phase separated by thin liquid films called lamellae can decrease mobility ratio between displacing and displaced fluids and address gravity segregation[4-6]. Foam modifies mobility ratio in two ways: first, the relative permeability of the displacing fluid (K_{rD}) decreases by trapping gas in porous media, and second, by increasing the effective shear viscosity of the displacing fluid (μ_{rD})[7]. Increase in apparent viscosity by foam comes from three contributions: (1) surface tension gradient created when surfactant foaming agent migrates from the front of the bubbles and accumulates at their back, (2) the thin liquid slugs between bubbles, and wall and bubbles, and (3) resistance to deformation of air bubbles pass through the porous media that have smaller size than foam bubbles[8]. Foam forms inside the porous media by three mechanisms leave behind, snap-off, and lamellae division. Leave behind is the dominant mechanism of foam generation at lower flow rates. As gas invades into a media saturated with surfactant, the lamellae are left behind the gas[9]. Snap off mechanism is more important at high flow rate and

can reduce the mobility of foam more significantly in comparison to the leave behind mechanism. Gas bubble expands as it moves through a pore throat to a pore body causing a decrease in capillary pressure and a pressure gradient in the liquid phase. Consequently, liquid accumulates in the pore throat and if the capillary pressure is large enough the liquid finally snaps off the gas bubble[10]. Lamellae division is similar to snap off and occurs at high flow rates. As a pre-existing lamellae approaches a branch point in porous media it divides into several lamellae[11]. Foam flows in porous media as a continuous phase or discontinuous phase[12]. Continuous flow occurs when gas goes through porous media without interruption by lamella. In discontinuous mode, gas is transferred as a chain of gas bubbles that are separated by lamella.

Foam can be placed in the reservoir by pre-generated foam injection, co-injection of gas and surfactant and surfactant-alternating-gas (SAG) injection. Surfactant must be used as the liquid phase to stabilize lamellae. Researches showed SAG injection in which alternating slugs of a surfactant solution and gas are injected into the reservoir is the optimum method for foam placing into the reservoir[13-15]. It reduces the contact of gas and water in surface facilities. More importantly, foam weakens as the gas displaces water from the near well-region and the injectivity of gas increases and the possibility of reservoir fracturing decreases[5, 16]. Holt and Vassenden[6] showed foam injection resulted in higher segregation length (i.e. a longer distance over which segregation occurs as a result of gravity) than gas and water. They showed that the following equation which was proposed by Stone[1] and Jenkins[17] can be used for calculating

segregation length (L_g) in SAG injection process (the distance over which segregation occurs as a result of gravity):

$$L_g = \frac{Q}{K(\rho_w - \rho_g) g D \gamma_{rt}^m} \quad (1)$$

where $Q(\frac{m^3}{s})$ is the total volumetric injection rate of gas and liquid, $K(m^2)$ is the vertical permeability of the porous medium, ρ_w and $\rho_g(\frac{kg}{m^3})$ are liquid and gas density respectively, $g(\frac{m}{s^2})$ is the gravity acceleration, $D(m)$ is the thickness of the porous medium, and $\gamma_{rt}^m = \frac{K_{rw}}{\mu_w} + \frac{K_{rg}}{\mu_g}(\frac{1}{Pa.s})$ is the total relative mobility of the mixed gas-liquid zone. Here K_{rw} and K_{rg} are relative permeability of water and gas respectively, and $\mu_w(Pa.s)$ and $\mu_g(Pa.s)$ are the viscosity of water and gas respectively. Shi and Rossen[5] indicated high value of gravity numbers (e.g. ratio between viscous and gravity forces) defined as $N_g = \frac{\Delta\rho.g}{\nabla p}$ promote gravity segregation in SAG injection process. Here ∇p ($\frac{Pa}{m}$) is the pressure gradient, $\Delta\rho(\frac{kg}{m^3})$ is the density differences between fluids and $g(\frac{m}{s^2})$ is the gravity acceleration. Some other researchers studied the effect of gravity segregation in SAG injection process[18-22]. However, they did not consider the effect of fingering of highly mobile gas into the foam bank in their studies. Recently, Farajzadeh et al[23]

showed in a simulation study that the fingering of highly-mobile gas into the foam bank may be unavoidable and causes instabilities in a foam injection process. This fingering can also distort the foam front, even when favorable mobility control creates in foam front. To the best of our knowledge, there is no experimental study to support these findings or refute them.

In this work, fingering of highly mobile gas into the foam bank and gravity segregation effects on fluids separation were studied in a foam injection process using a 2D micromodel system at a wide range of the injection rate.

Experimental Considerations

Design and fabrication of porous media

Following the procedure described by Osei-Bonsu et al.[24], the porous medium used in this research was designed with 'Rhinoceros' CAD software package for 3D illustrations. The pore network was created from a Voronoi diagram consisting of 660 polygons. Voronoi diagrams can be used to design homogenous and heterogeneous microfluidic and micromodel network that was used in many theoretical and numerical studies in the field of porous media and also commonly used in the foams literature[25-27]. The model was populated with a random length pore throat size distribution ranging from 0.3 to 0.5 mm. The pore throat size can be defined as the radius of a circle fitting in the narrowest space that connect two adjacent pore bodies together. Figures 1 (a), (b) and (c) show the top view of the porous medium, a zoomed portion of the model and the pore throat size distributions of the model, respectively. The dimension of the printed matrix was 110 mm x

50 mm x 0.25 mm. The model was oil wet and the porosity and permeability of the model were 39.4 % and 10.6 Darcy, respectively. The stereolithographic (STL) file of the CAD model was printed with an acrylic based material (acrylic oligomer) using a high resolution Polyjet 3D printer (Objet 30 pro, Stratasys, UK). The top of the model was sealed with a Plexiglas plate to prevent flow over the grains. Furthermore, two perforations (1 mm diameter) at opposite ends of the porous medium were placed to serve as the inlet and outlet.

Fluid properties and experimental procedure

In each run of the experiment, the printed porous medium was saturated with Isopar V (Brenntag, UK) referred to as 'oil' hereafter. The oil was stained red in order to enhance the visual contrast. Table 1 shows properties of the oil used in this study.

Table 1. Properties of the oil together with its surface tension and interfacial tension with the surfactant solution used in the present study[2, 28].

Oil	Composition	Viscosity (x 10^{-3} Pa.s)	Density (g/cm^3)	Surface tension (mN/m)	Interfacial tension (mN/m)
Isopar V	C14-C19	10.84	0.81	25.44	0.13

The surfactant solution used for foam generation was prepared from a 1:1 blend of sodium dodecyl sulphate and cocamidopropyl betaine (2% active content) with 0.25M NaCl solution. Osei-Bonsu et al. [28] showed that this surfactant combination was tolerant to the presence of oil under our experimental conditions. The surfactant solution and nitrogen were injected using a syringe pump (Harvard Apparatus, PhD Ultra) and a mass flow controller (Bronkhorst, UK).

Surfactant and gas met before the model and flowed into the model as intermittent slugs of surfactant and gas.

A high-resolution digital camera (Teledyne DALSA Genie) controlled by a computer was used to acquire images of the displacement process at regular time intervals. The model porous medium was placed adjacent to a light box to improve the illumination of the captured images. The recorded images had a resolution of 2560 x 2048 pixels with 8 bit gray levels resulting in the pixel size of 40 microns.

To understand the effect of fingering of high mobile gas into the foam bank and gravity segregation on fluids separation, we conducted experiments in horizontal and vertical orientations in a printed porous medium. In all experiments, foam was generated in-situ by intermittent injection of gas and surfactant slugs at six flow rates of 1, 5, 10, 20, 40 and 80 ml/hr. The fraction of surfactant in injection fluids was 15% of the total volume injected in all experiments. Each run of the experiment was repeated at least three times to ensure the reproducibility of the data. The error bars in the following figures represent the variability in the obtained results for each kind of experiments.

Image analysis

The recorded images were analyzed using in-house codes developed in MATLAB to distinguish the oil, grains (solid phase) and the injected fluids (see Osei-Bonsu et al.[24] for details of the segmentation algorithm). Additionally, Image J software was used to determine

the number of oil blobs due to the fragmentation of the oil phase. Figure 1 (d) and (e) illustrate a typical recorded image and its corresponding segmented image.

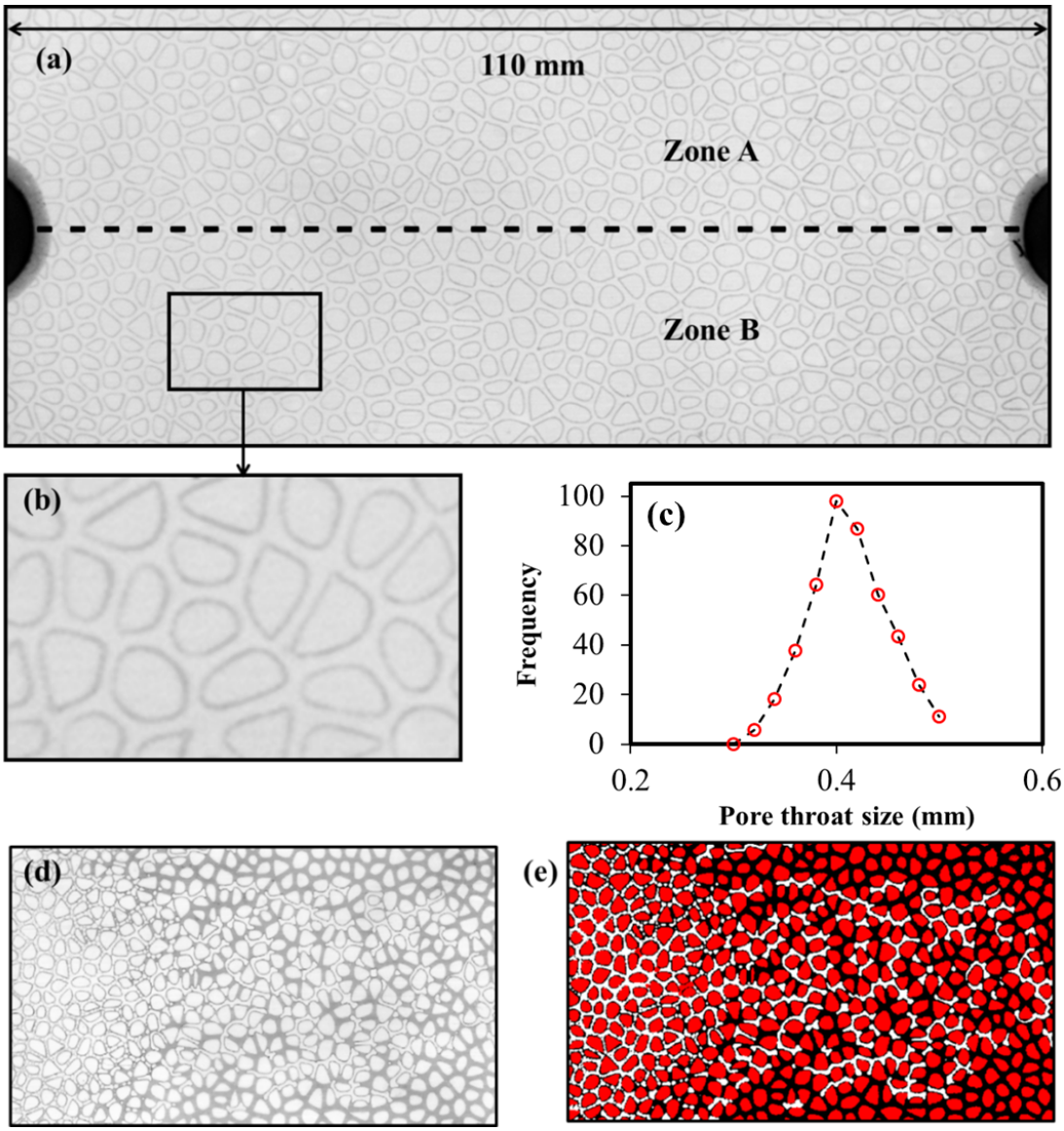

Figure. 1 (a) Top view of the printed model used in our study. The upper and lower part of the model is referred as Zone A and Zone B in the following analysis. (b) Magnified image of pores to better illustrate the patterns of pores/grains in the printed porous medium (c) Pore throat size distribution of the printed porous medium. (d) A typical image recorded during oil displacement by foam. Dark grey represents oil. (e) The corresponding segmented image of

the phase distributions presented in (d) with white, black and red representing foam (or escaping gas and surfactant), oil and grain respectively.

RESULTS AND DISCUSSION

Effects of gas fingering and gravity segregation on foam displacement efficiency

Figure 2 presents oil recovery in the case of horizontal and vertical orientations at different pore volume injected under different injection rates. The recovery factor is defined as the fraction of oil initially in place that is produced during the injection process after a given number of pore volumes have been injected.

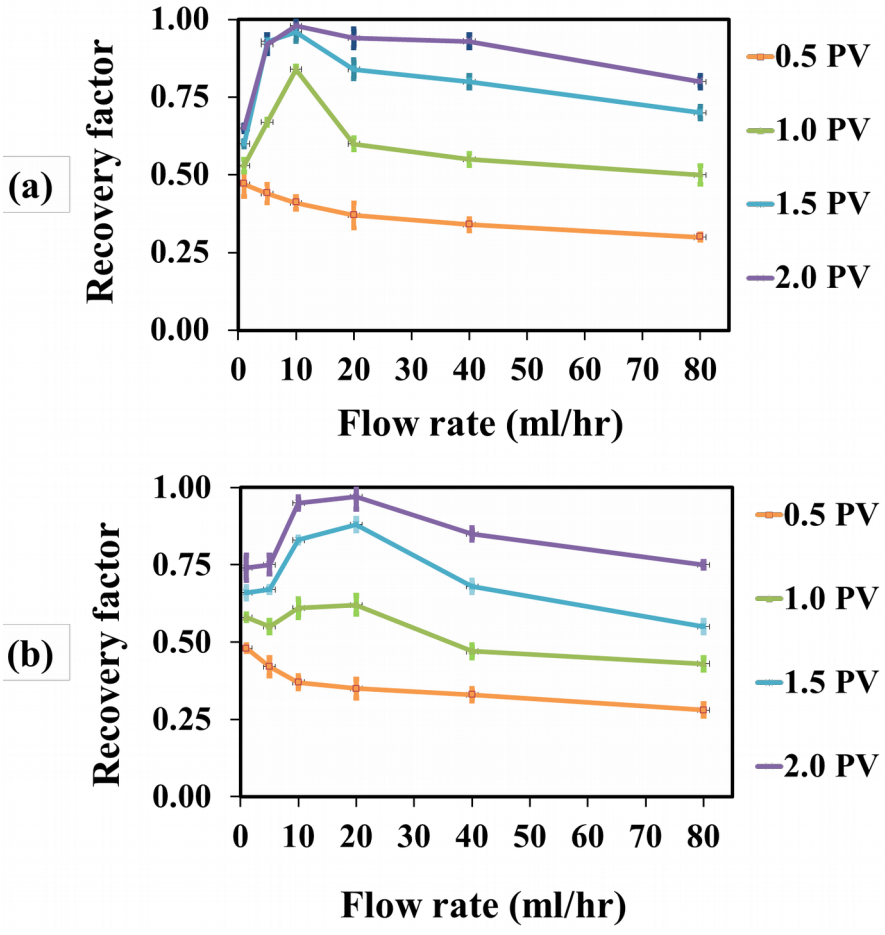

Figure. 2 Oil recovery in the (a) horizontal and (b) vertical orientations, respectively as a function of the flow rate at different pore volume injected indicated in the legend.

According to the Figure 2, three distinct flow regimes are detectable in both vertical and horizontal orientations depending on the applied injection rate. The characteristics of each flow regime are discussed in the following. For better understanding the nature of each flow regime, phase distribution and pressure drop corresponding to each flow regime are presented in Figure 3.

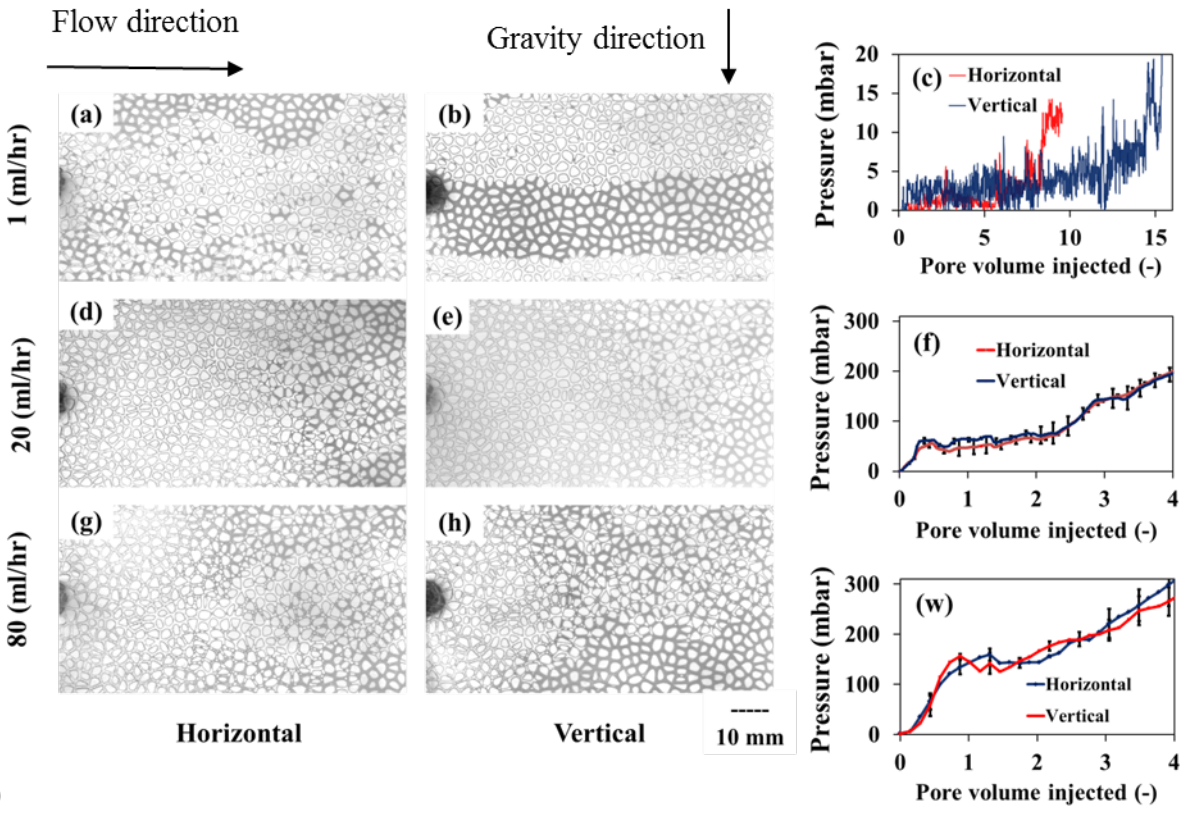

Figure. 3 Phase distribution in horizontal and vertical orientations at different flow rates. (a), (d) and (g) correspond to the horizontal orientation and (b), (e), and (h) corresponds to the vertical orientation. (c), (f) and (w) illustrate the measured pressures in the case of horizontal and vertical orientation at the flow rate of 1, 20 and 80 ml/hr, respectively.

Horizontal orientation

Applying low injection rate (1 ml/hr) impacted lamellae generation and mobilization and subsequently displacement efficiency. Visual inspections at this flow regime showed limited rate of lamellae generation. Lamellas were created by leave behind mechanism and snap-off and stayed stagnant. According to Rossen and Gauglitz[29] a minimum pressure gradient required for lamellae generation and mobilization that was not achieved initially at this flow regime. It was observed gas tended to be trapped behind lamellae in some point until the pressure drop per lamella built up and passed the threshold for mobilization. After mobilization, the pressure drop of the model decreased and lamellae destruction occurred when the moving lamellae met the oil phase. The fluctuations in the recorded pressures observed in Figure 3 (c) are due to the unsteady state nature of the displacement process (i.e. lamella generation leads to increase the pressure and lamella mobilization and coalescence leads to pressure reduction). Capillary numbers (e.g. ratio between viscous and gravity forces, $Ca=\frac{\mu.v}{\sigma}$) were calculated for each set of experiments in Table 2. Here $\mu(Pa.s)$ is the viscosity of the injected fluids (due to most of the injected fluids was gas, viscosity of gas was used in the calculations), $v(\frac{m}{s})$ is the total superficial velocity of the injected fluids, and $\sigma(\frac{N}{m})$ is the surface tension between gas and surfactant. Low value of capillary number at low flow rate in horizontal orientation is associated with low rate of lamellae generation and mobilization.

Table 2. Capillary numbers for the experiments conducted at different flow rates.

Flow rate (ml/hr)	Ca
1	1.4×10^{-6}
5	7.2×10^{-6}
10	1.4×10^{-5}
20	2.9×10^{-5}
40	5.8×10^{-5}
80	1.1×10^{-4}

The limited rate of lamellae generation and mobilization and the existence of lamellae destruction resulted in establishing a weak foam in the model. Figure 4 shows low value of

apparent viscosity at low flow rate associated to limited rate of foam generation. Full oil recovery achieved after 10 PV injections and the residing oil displaced mostly by gas and surfactant instead of foam. High rate of lamellae generation and mobilization was observed after 6 PV of injection as the pressure gradient increased and the oil saturation decreased. After adequate fluids injection, the whole model was saturated with foam bubbles. According to table 2, this flow regime is corresponding to capillary numbers lower than about 1.0×10^{-6}.

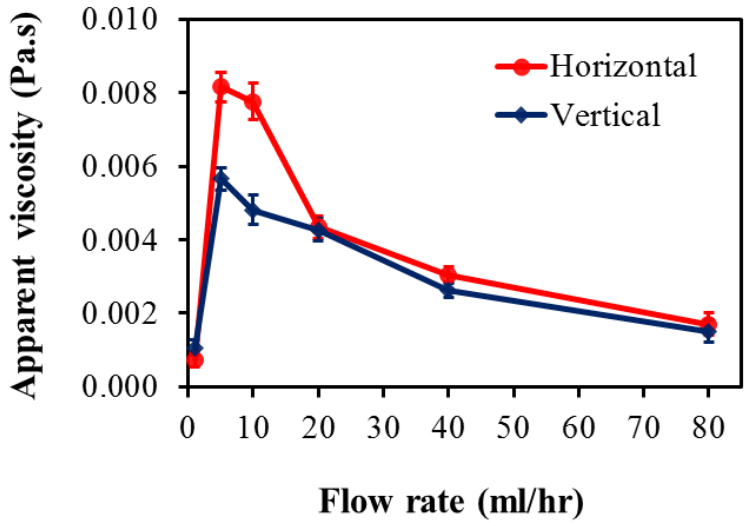

Figure. 4 The relationship between apparent viscosity of foam and flow rate after 4 PV of injection process.

The second flow regime occurred when the pressure gradient is large enough to produce fine textured foams generated mostly by snap-off mechanism and lamella division. The rate of lamellae generation and mobilization was large enough to make strong foam as can be seen in Figure 4. The gradual increase in the pressure drop and less pressure fluctuations in Figure 3 (f) confirmed strong foam generation. Fingering of the gas phase through the foam bank was however observed in this flow regime such that a continuous gas phase was formed inside the

model. In addition, Gas released from foam coalescence fingered through the oil phase in front of it and created some isolated oil blobs as can be seen in Figure 3 (d). In this flow regime, full oil recovery from the porous medium was attained after approximately 2.5 PV of injection.

At high flow rates, the displacement efficiency of foam injection decreased again as can be seen in Figure 2 (a) and Figure 3 (g). This is due to that at higher injection flow rate, more volume of gas fingers and subsequently more escaping gas occurred as can be seen in Figure 5. Visual observations also showed the volume of foam that existed as continuous phase increases by increasing flow rate. This continuous gas phase eventually fingered through the oil phase. Fingering more volume of gas caused instability in the displacement process and decrease in displacement efficiency. It may be expected that this gas fingering is due to dry-out effect of foam at 85 foam quality. It can be said the dry-out effect is not relevant in our system with rather larger pores. Also, Kofi Osei-Bonsu et al [24] used the same surfactant and a porous media quite similar to what we used in our study and found the foam quality corresponds to the critical capillary pressure was 98. Therefore, we can be sure that in our system, it is presumably the presence of oil (rather than the dry out effect) which is what helps to destabilise foam. Complete oil displacement was occurred after about 3.5 PV of injection at 80 ml/hr flow rate.

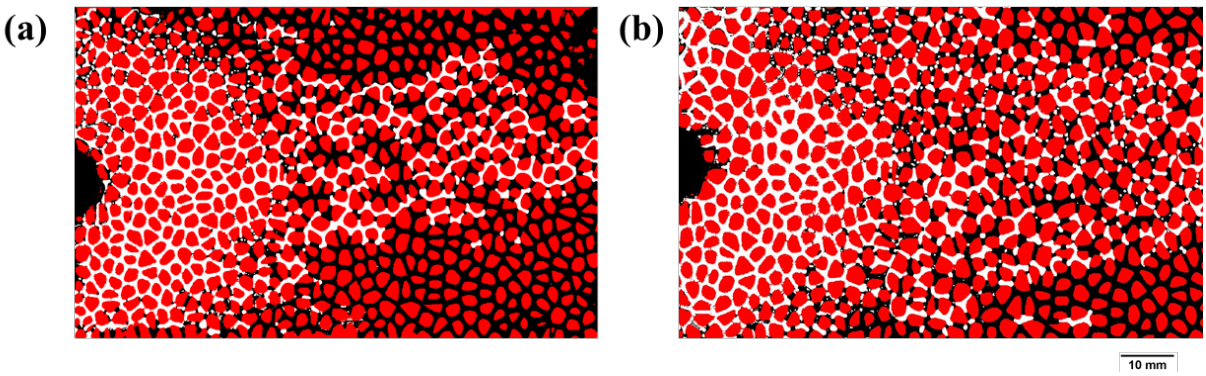

Figure. 5 (a) and (b) show phase distribution for 20 and 80 ml/min gas flow rate respectively I in horizontal orientation.

Vertical orientation

Similar to the horizontal orientation, three distinct flow regimes were observed in the case of the vertical orientation. The first flow regime includes the lower end of injection rates (from 1 ml/hr to 5 ml/hr). Complete segregation of gas and surfactant was the dominant characteristic of this flow regime as depicted in Figure 3 (b). As Shi and Rossen proposed [5] large values of gravity number imply gravity segregation. Here gravity number ($N_g = \frac{\Delta \rho . g}{\nabla P}$) was calculated for different flow rates after 1 PV injection in Table 3 for the experiment conducted in vertical orientation.

Table 3. Calculated Gravity number for the experiments conducted at different flow rates in vertical orientation after 1 PV injection.

Flow rate (ml/hr)	N_g

1	1.5×10^{-1}
5	2.7×10^{-2}
10	7.3×10^{-3}
20	4.3×10^{-3}
40	2.4×10^{-3}
80	1.45×10^{-3}

At low flow rate, flow rate was not large enough to provide a proper mixing zone for foam generation. Upon entering the model, gravity segregation occurred resulting from the density differences between the fluids: gas flowed upward (Zone A) while the surfactant flowed downward (Zone B) in the model. Therefore, oil was displaced predominantly by gas in Zone A and by surfactant in Zone B. The upper and lower part of the model is referred as Zone A and Zone B as depicted in Figure 1 (a). Complete oil recovery was achieved after 16 PV owing to the adverse impact of the high gravity segregation on fluids separation. Foam generation was started after 12 PV of injection mostly by leave behind mechanism. After many pore volume fluids injections, the whole model was saturated with foam. Based on Table 3, high gravity segregation occurred at gravity number more than 1.0×10^{-2}.

The second flow regime corresponds to the intermediate injection rates. According to equation (1), increasing flow rate leads to longer mixed zone and thus more foam generation

and increase in apparent viscosity of foam as depicted in Figure 4. Segregation length L_g can be estimated by combining Darcy's law with equation (1) which leads to $L_g = \left(\frac{\Delta P_{Horizontal}}{\Delta P_{Hyd}}\right)\left(\frac{W.D}{L}\right)$ that W, D and L are the width, thickness and length of the porous medium. The hydrostatic pressure ($\Delta P_{Hyd} = \rho g W$) across the model porous medium with W=50 mm in height gives rise to an approximate pressure of 4 mbar. Assuming a horizontal pressure drop of 100 mbar (Figure 3 (f)), the segregation length will be in the order of 3 mm. The recorded images showed that the foam generation mostly occurred at this segregation length followed by foam propagation to other parts of the porous medium as illustrated in Figure 3 (e). Beside foam generation in the mixed zone, the movement of gas to Zone A and surfactant to Zone B was observed. The accumulation of surfactant in Zone B provided suitable condition for generating lense in Zone B by leave behind mechanism.

The third regime in the case of vertical orientation corresponds to the higher injection rates. In this flow regime, foam was generated in the mixed zone. However, similar to horizontal orientation, fingering of high volume of gas had adverse effect on foam displacement as can be seen in Figure 3 (h). Although, higher flow rates helped with addressing the effect of gravity segregation, but displacement efficiency decreases due to gas viscous fingering.

Quantitative analysis on foam saturation

The analysis presented above highlighted the adverse effect of gas fingering and fluids separation by gravity segregation on foam bank saturation. Our recorded images of oil

displacement by foam in porous media enabled us to measure the area of porous media saturated by foam. Figure 6 (b) illustrates foam saturations at different flow rates after 1.2 PV injections for both horizontal and vertical orientations. Foam saturation was calculated by dividing the area occupied by foam to the total area of the pore space. The recorded images were segmented to calculate the area covered by the foam bubbles. A typical example of the segmented image is illustrated in Figure 6 (a). The solid blue line in Figure 6 (a) indicates the foam front. The white color to the right side of the foam front corresponds to the gas phase escaping out of foam due to gas fingering or the coalescence of foam bubbles by oil which was not included in the calculation of foam saturation.

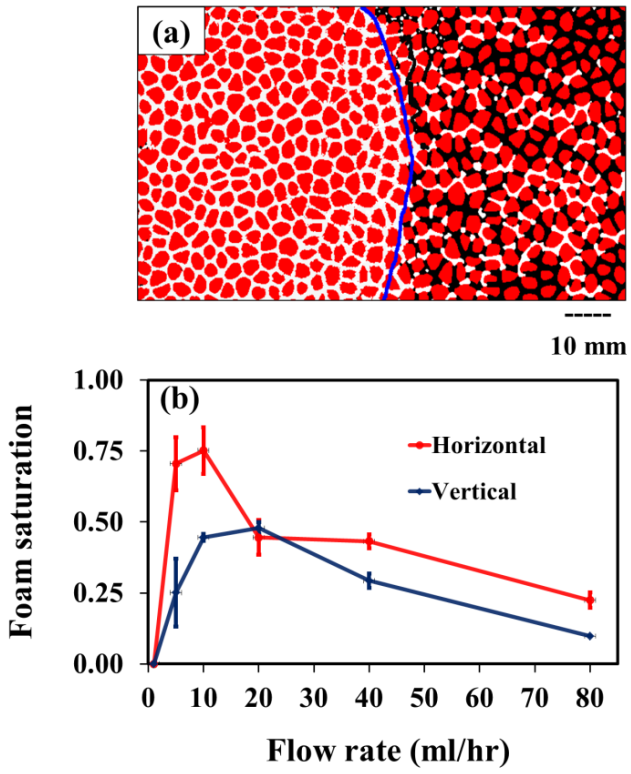

Figure. 6 (a) A typical segmented image used for calculating the saturation of foam. Red, black and white indicate the grains, oil and foam (and escaping gas) respectively. This image corresponds to the case of 10 ml/hr injection rate in the horizontal orientation. (b)

Relationship between the flow rate and foam saturation after 1.5 PV injection of gas and surfactant solution for the horizontal and vertical orientation. The error bars indicate the standard deviation over 3 repeat measurements.

In the horizontal orientation, after 1.2 PV injection and when the injection rate is low (first flow regime), due to low rate of lamellae generation and mobilization and existence of lamellae destruction there was no foam and hence foam saturation was zero. Then foam saturation increased in the second flow regime (the intermediate stage) to about 75 percent as foam generation by snap off mechanism increased. In the third flow regime, the saturation of foam influenced by gas fingering and decreased to about 25 percent.

In the vertical orientation, the saturation of foam was zero in the first flow regime (when the injection rate is low) due to complete segregation of gas and surfactant. In the second flow regime, the effect of gravity segregation decreased by increasing flow rate leading to increasing foam saturation (around 50 percent) followed by the third flow regime (when the injection rate is high) where the saturation of foam decreases to about 15 percent resulted from gas fingering.

Effects of the injection rate and gravity segregation on oil entrapment

Our results indicated that gas fingering and fluids separation by gravity segregation has significant impact on the oil entrapment and spatial distribution of the oil blobs during foam flooding in porous media. Using the recorded images, we computed the number of

disconnected oil phase in Zone A and Zone B (defined in Figure 1) with the results presented in Figure 7.

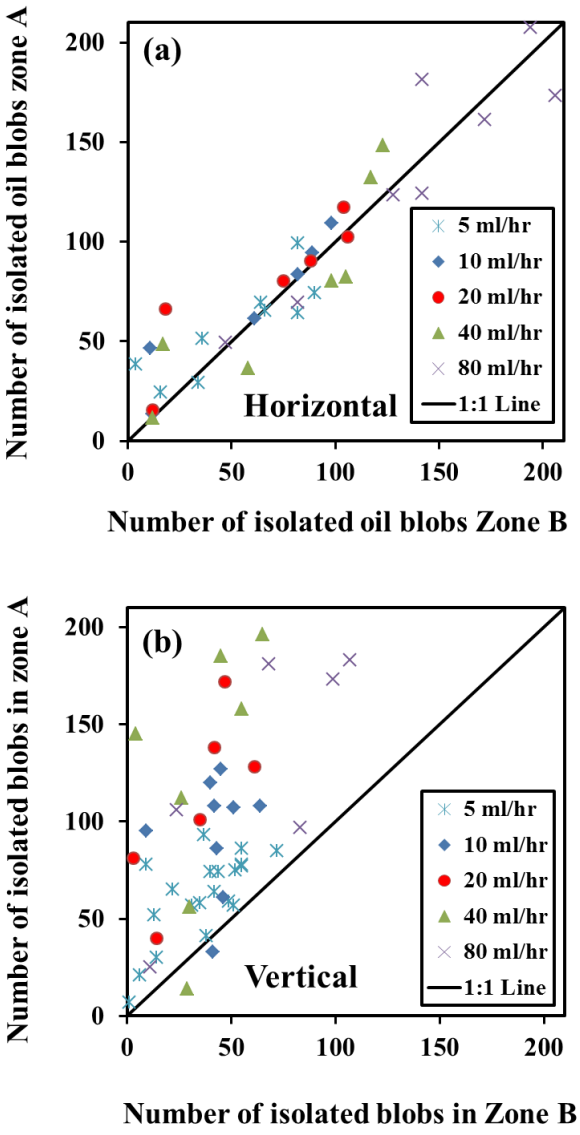

Figure. 7 The relationship between the number of trapped oil blobs in Zone A and Zone B in (a) horizontal and (b) vertical orientation, respectively. The legend indicates the applied injection rates.

Figure 7 (a) shows the oil blob distribution through the horizontal model porous medium is almost homogenous with nearly similar number of isolated oil blobs distributed in Zone A

and Zone B (defined in Figure 1). However, this is not the case when the porous medium is placed vertically with most of the blobs trapped within Zone A (i.e. the upper part of the porous medium). As already illustrated, during injection through the vertical oriented porous medium, gas and surfactant solution moved to Zone A and Zone B, respectively due to the gravity segregation. Since the viscosity contrast between gas and oil is greater than viscosity contrast between surfactant and oil, Zone A is more prone to fingering and formation of isolated oil blobs. One can add to this the contribution of the fraction of gas escaping from Zone B toward Zone A due to the gravity.

Dynamics of foam displacement influenced by the gravity

In addition to the number and distribution of oil blobs, oil recovery and foam saturation, gravity segregation influences the dynamic of foam front displacement. As an example, Figure 8 qualitatively shows the patterns and dynamics of foam front displacement at 10 ml/hr injection rate in the case of horizontal and vertical porous medium.

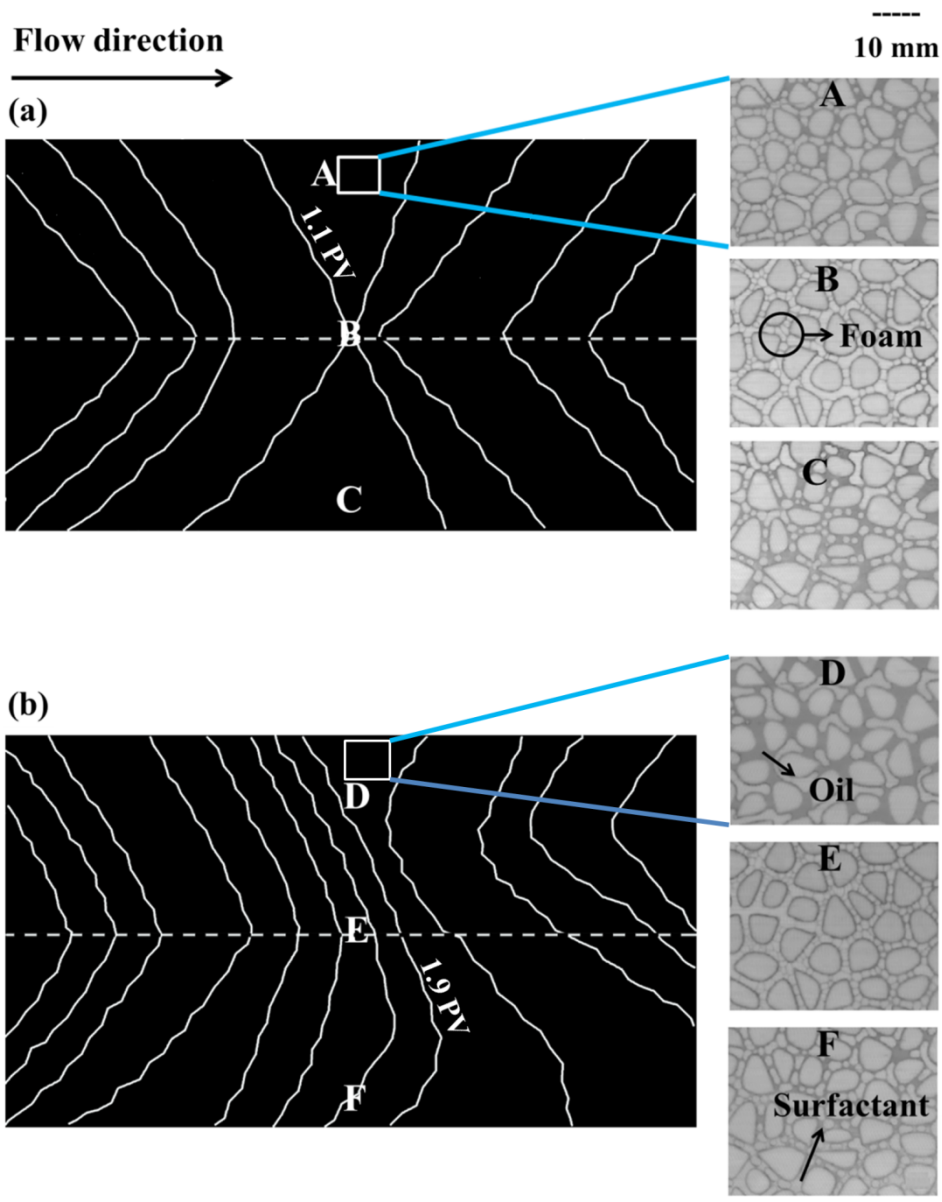

Figure. 8 The interface (white line) between invaded and uninvaded area at the equal pore volume injected intervals of 0.2 in the porous medium placed (a) horizontally and (b) vertically. The interface propagates from left to right. The first interface at the left side of the figure corresponds to 0.5 PV injected. The injection rate in both cases was fixed at 20 ml/hr. The dashed line is the boundary between Zone A and Zone B. The insets illustrate typical examples of phase distribution at upper, middle and lower parts of the porous medium.

During oil displacement in horizontal orientation, the front had a convex shape up to 1.2 PV injection followed by a gradual evolution into a concave front. The morphological evolution of the front is likely due to variations in the foam texture along the front. The insets in Figure 8 illustrating typical phase distribution patterns at the upper, middle and lower regions of the porous medium placed horizontally shows that the bubble density in the middle region is higher than upper and lower regions. Higher bubble density decreases the mobilization of foam bubbles in the middle section of the model thus diverting the flow to the upper and lower regions which causes the change in the morphology of the front.

In vertical orientation, foam front adopted an 'S' shape after 1.7 PV injections. This is due to the gradual increase of the bubble density in the middle region and that a small part of Zone A caused high flow resistance (this is once again due to high bubble density) and changed flow orientations to other parts of the model. Subsequently, the foam front propagation in Zone B was faster than Zone A due to the presence of more liquid in Zone B (higher saturation) compared to Zone A as a result of the gravity segregation which led to a decrease in flow resistance in that region.

Summary and conclusions

This study set out to investigate the effects of fingering of highly mobile gas into the foam bank and gravity segregation on fluids separation on the performance of foam injection process. A comprehensive series of foam injection experiments were conducted in both horizontal and vertical orientations in a porous medium fabricated by 3D printing technology in the presence of oil. In horizontal orientation, obtained results showed lamellae generation

and mobilization was not large enough at capillary number below 10^{-6} to generate strong foam. Increasing flow rate led to generation of fine textured foam by snap off mechanism. However, gas fingering into the oil bank influence foam injection process and had adverse effect on displacement efficiency at higher flow rate. In vertical direction, complete segregation of gas and surfactant occurred at gravity number higher than 1.0×10^{-2}. A rise in flow rate led to increase in foam generation in the mixed zone and addressing gravity segregation. However, gas viscous fingering at high flow rates resulted in a decrease in foam sweep efficiency. These findings highlight the significant adverse impact of gas fingering and gravity segregation on foam performance echoing the necessity to include these phenomena when investigating flow displacement by foam in porous media.

ACKNOWLEDGMENT

We would like to acknowledge the UK Engineering and Physical Sciences Research Council (EPSRC) to provide the PhD studentship for Mohammad Javad Shojaei. We thank Mr. Andrew Evans, Mr. Ian Small and Mr. Craig Shore for their assistance with the experimental setup.

REFERENCES

(1) Stone, H. L. *Vertical conformance in an alternating water-miscible gas flood*; Exxon Production Research Co.: 1982.

(2) Spivak, A., Gravity segregation in two-phase displacement processes. *Society of Petroleum Engineers Journal* 1974**,** 14, (06), 619-632.

(3) Zendehboudi, S.; Chatzis, I.; Mohsenipour, A. A.; Elkamel, A., Dimensional analysis and scale-up of immiscible two-phase flow displacement in fractured porous media under controlled gravity drainage. *Energy & Fuels* 2011**,** 25, (4), 1731-1750.

(4) Kibodeaux, K.; Rossen, W. In *Coreflood study of surfactant-alternating-gas foam processes: Implications for field design*, SPE Western Regional Meeting, 1997; Society of Petroleum Engineers: 1997.

(5) Shi, J.; Rossen, W. In *Improved surfactant-alternating-gas foam process to control gravity override*, SPE/DOE improved oil recovery symposium, 1998; Society of Petroleum Engineers: 1998.

(6) Holt, T.; Vassenden, T. In *Reduced gas-water segregation by use of foam*, IOR 1997-9th European Symposium on Improved Oil Recovery, 1997; 1997.

(7) Zhu, T.; Ogbe, D.; Khataniar, S., Improving the foam performance for mobility control and improved sweep efficiency in gas flooding. *Industrial & engineering chemistry research* 2004**,** 43, (15), 4413-4421.

(8) Hirasaki, G.; Lawson, J., Mechanisms of foam flow in porous media: apparent viscosity in smooth capillaries. *Society of Petroleum Engineers Journal* 1985**,** 25, (02), 176-190.

(9) Hematpour, H.; Mahmood, S. M.; Nasr, N. H.; Elraies, K. A., Foam flow in porous media: Concepts, models and challenges. *Journal of Natural Gas Science and Engineering* 2018.

(10) Ransohoff, T.; Radke, C., Mechanisms of foam generation in glass-bead packs. *SPE reservoir engineering* 1988**,** 3, (02), 573-585.

(11) Dicksen, T.; Hirasaki, G. J.; Miller, C. A. In *Conditions for foam generation in homogeneous porous media*, SPE/DOE Improved Oil Recovery Symposium, 2002; Society of Petroleum Engineers: 2002.

(12) Falls, A.; Hirasaki, G.; Patzek, T. e. a.; Gauglitz, D.; Miller, D.; Ratulowski, T., Development of a mechanistic foam simulator: the population balance and generation by snap-off. *SPE reservoir engineering* 1988**,** 3, (03), 884-892.

(13) Ma, K.; Liontas, R.; Conn, C. A.; Hirasaki, G. J.; Biswal, S. L., Visualization of improved sweep with foam in heterogeneous porous media using microfluidics. *Soft Matter* 2012**,** 8, (41), 10669-10675.

(14) Kloet, M.; Renkema, W. J.; Rossen, W. R. In *Optimal design criteria for sag foam processes in heterogeneous reservoirs*, EUROPEC/EAGE conference and exhibition, 2009; Society of Petroleum Engineers: 2009.

(15) Holm, L., Foam injection test in the Siggins field, Illinois. *Journal of Petroleum Technology* **1970,** 22, (12), 1,499-1,506.

(16) Xu, Q.; Rossen, W. In *Experimental study of gas injection in surfactant-alternating-gas foam process*, SPE annual technical conference and exhibition, 2003; Society of Petroleum Engineers: 2003.

(17) Jenkins, M. In *An analytical model for water/gas miscible displacements*, SPE enhanced oil recovery symposium, 1984; Society of Petroleum Engineers: 1984.

(18) Hussain, A.; Amin, A.; Vincent-Bonnieu, S.; Farajzadeh, R.; Andrianov, A.; Hamid, P. A.; Rossen, W. In *Effect of Oil on Gravity Segregation in SAG Foam Flooding*, IOR 2017-19th European Symposium on Improved Oil Recovery, 2017; 2017.

(19) Rossen, W. R.; Van Duijn, C.; Nguyen, Q. P.; Shen, C.; Vikingstad, A. K., Injection strategies to overcome gravity segregation in simultaneous gas and water injection into homogeneous reservoirs. *SPE Journal* **2010,** 15, (01), 76-90.

(20) Faisal, A.; Bisdom, K.; Zhumabek, B.; Zadeh, A. M.; Rossen, W. R. In *Injectivity and gravity segregation in WAG and SWAG enhanced oil recovery*, SPE Annual Technical Conference and Exhibition, 2009; Society of Petroleum Engineers: 2009.

(21) Renkema, W.; Rossen, W. In *Success of SAG foam processes in heterogeneous reservoirs*, IPTC 2007: International Petroleum Technology Conference, 2007; 2007.
(22) Rossen, W. R.; Van Duijn, C.; Nguyen, Q. P.; Vikingstad, A. K. In *Injection strategies to overcome gravity segregation in simultaneous gas and liquid injection in homogeneous reservoirs*, SPE/DOE symposium on improved oil recovery, 2006; Society of Petroleum Engineers: 2006.
(23) Farajzadeh, R.; Eftekhari, A.; Hajibeygi, H.; Kahrobaei, S.; Van der Meer, J.; Vincent-Bonnieu, S.; Rossen, W., Simulation of instabilities and fingering in surfactant alternating gas (SAG) foam enhanced oil recovery. *Journal of Natural Gas Science and Engineering* 2016**,** 34, 1191-1204.
(24) Osei-Bonsu, K.; Grassia, P.; Shokri, N., Investigation of foam flow in a 3D printed porous medium in the presence of oil. *Journal of colloid and interface science* 2017**,** 490, 850-858.
(25) Wu, M.; Xiao, F.; Johnson-Paben, R. M.; Retterer, S. T.; Yin, X.; Neeves, K. B., Single-and two-phase flow in microfluidic porous media analogs based on Voronoi tessellation. *Lab on a Chip* **2012,** 12, (2), 253-261.
(26) Weaire, D.; Kermode, J., Computer simulation of a two-dimensional soap froth: I. Method and motivation. *Philosophical Magazine B* 1983**,** 48, (3), 245-259.
(27) Weaire, D.; Kermode, J., The evolution of the structure of a two-dimensional soap froth. *Philosophical Magazine Part B* 1983**,** 47, (3), L29-L31.
(28) Osei-Bonsu, K.; Shokri, N.; Grassia, P., Foam stability in the presence and absence of hydrocarbons: From bubble-to bulk-scale. *Colloids and Surfaces A: Physicochemical and Engineering Aspects* 2015**,** 481, 514-526.
(29) Rossen, W.; Gauglitz, P., Percolation theory of creation and mobilization of foams in porous media. *AIChE Journal* **1990,** 36, (8), 1176-1188.